Journal of Hazardous Materials 185 (2011) 922–929

Contents lists available at ScienceDirect

Journal of Hazardous Materials

journal homepage: www.elsevier.com/locate/jhazmat

Pb(II) and Cd(II) biosorption on *Chondracanthus chamissoi* (a red alga)

Andrea Yipmantin[a,b], Holger J. Maldonado[b], Martha Ly[b], Jean Marie Taulemesse[c], Eric Guibal[a,*]

[a] *Ecole des Mines d'Alès, Laboratoire Génie de l'Environnement Industriel, 6 avenue de Clavières, F-30319 Ales cedex, France*
[b] *Universidad Peruana Cayetano Heredia, Departamento Académico de Química, Av. Honorio Delgado, 430 Urb. Ingeniería, San Martín de Porres, Lima, Peru*
[c] *Ecole des Mines d'Alès, Centre des Matériaux de Grande Diffusion, 6 avenue de Clavières, F-30319 Ales cedex, France*

ARTICLE INFO

Article history:
Received 23 June 2010
Received in revised form 24 August 2010
Accepted 28 September 2010
Available online 7 October 2010

Keywords:
Chondracanthus chamissoi
Lead
Cadmium
Sorption isotherms
Uptake kinetics

ABSTRACT

Chondracanthus chamissoi is an efficient biosorbent for Pb(II) and Cd(II). The sorption efficiency increases with pH and reaches an optimum around pH 4. Maximum sorption capacity reaches 1.37 mmol Pb g^{-1} and 0.76 mmol Cd g^{-1}. The biosorbent has a marked preference for Pb(II) over Cd(II), though insufficient for separating these metals by a simple sorption step. The uptake kinetics is controlled by the resistance to intraparticle diffusion with a limited impact of particle size, metal concentration and sorbent dosage. In the present case, grinding the biomass does not improve sorption capacity and uptake kinetics. The sorption of metal ions is probably due to their interaction with carrageenan (one of the main constituents of the biosorbent): sulfonic groups (on the sulfated polysaccharide) have a higher affinity for Pb(II) than for Cd(II) according to HSAB rules.

1. Introduction

The regulations concerning wastewater discharge to the environment are becoming more and more drastic in order to recycle waste streams and optimize the use of water resources. Effluents containing metal ions processing from mining, metallurgy activities are important sources of contamination of water bodies. Conventional processes for metal recovery include precipitation [1], solvent extraction [2], sorption on ion exchange, extractant impregnated and chelating resins [3,4]. Though these processes are globally efficient, they frequently face economical and/or technical limitations. Indeed, they may be non competitive for the treatment of low-concentration effluents (resins, solvent extraction), not capable of reaching requested levels of decontamination (precipitation). They may have serious environmental drawbacks since they can produce huge amounts of contaminated sludge (precipitation) or toxic compounds release (solvent extraction). The thermal degradation of synthetic resins at the end of their life cycle can also produce hazardous sub-products [5]. These are some reasons that can explain the interest of research community for developing alternative processes such as biosorption.

Biosorption consists in using materials of biological origin for the sorption of target molecules (metal ions, dyes, etc.) through interactions that mimic those involved in metal binding on ion exchange and chelating resins. Though most of the studies focus on living or non-living biomass (bacteria, fungi, yeast, etc.), sub-products from agriculture, marine industry have also been frequently cited as biosorbents [6,7]. Brown and green algae have retained most of the attention in the field of metal biosorption [8–14]. The presence of alginate in their cell wall may explain their high efficiency for metal uptake through complexation or ion exchange on carboxylic acid groups (guluronic and mannuronic acids). However, red algae may have also significant potential for sorption [15–18]. These algae are characterized by the presence of other polysaccharides like carrageenan. Actually, the term carrageenan recovers a number of different linear sulfated galactans. They are composed of alternating 3-linked β-D-galactopyranose (G-units) and 4-linked α-D-galactopyranose (D-units) or 4-linked 3,6-anhydro-α-D-galactopyranose (DA-units): these associations form the disaccharide repeating unit of carrageenan. Different carrageenans exist corresponding to different units, different arrangements and different proportions (Fig. AM1, in the Additional Material section) [19–21]. Carrageenan is used for its gelling properties in cosmetics, food industry, for coagulation and flocculation in environmental applications, for encapsulation in biotechnology. The sulfonic groups of the biopolymer are responsible for metal binding [22]: actually, the efficiency of the polymer depends on its degree of sulfatation.

Red algae can be considered as potential marine resource and in many countries of South America alga farming is considered a competitive activity for the production of carrageenan: *Chondracanthus chamissoi* has been cultivated for the extraction of this biopolymer [23,24]. The ability of this biomass for sorbing metals should be investigated not only for the potential of these biosorbents but

* Corresponding author. Tel.: +33 46 6782734; fax: +33 46 6782701.
E-mail addresses: eric.guibal@ema.fr, Eric.Guibal@mines-ales.fr (E. Guibal).

0304-3894/$ – see front matter © 2010 Elsevier B.V. All rights reserved.
doi:10.1016/j.jhazmat.2010.09.108

also for evaluating how these biosorbents could be at the origin of a contamination of carrageenan sources (for applications in food, cosmetics and health).

This study evaluates *C. chamissoi* for the sorption of Pb(II) and Cd(II). These metal ions are frequently found in wastewater from mining, metallurgy industries and may contribute to contaminate marine environment and local fauna and flora [25,26]. FT-IR spectrometry was used for characterizing the biopolymers extracted from the alga and the spectrum was compared to the spectra of ι- and κ-carrageenan. After investigating the impact of pH on metal sorption, the sorption isotherms were determined at optimum pHs and experimental curves were modeled using the Langmuir equation. Finally, the influence of a series of experimental parameters (particle size, sorbent dosage, and metal concentration) on uptake kinetics was investigated using the models of resistance to film diffusion and to intraparticle diffusion and the pseudo-second order rate equation for simulating kinetic profiles.

2. Materials and methods

2.1. Materials

Lead acetate trihydrate ($Pb(CH_3COO)_2{\cdot}3H_2O$, Carlo Erba) and cadmium chloride ($CdCl_2{\cdot}2.5H_2O$, Merck) salts were used for the preparation of stock solutions. Other solutions were prepared by dilution using Milli-Q demineralized water.

The red alga was collected in the Bahía de Chancay (Province of Huaral, Péru) in August 2009. It was identified as *C. chamissoi* (C. Agardh) Kützing. The material was abundantly rinsed with tap water and finally with demineralized water. The clean biomass was then dried at room temperature before being ground and sieved at the following sizes:

$$80\,\mu m < PS1 < 125\,\mu m < PS2 < 250\,\mu m < PS3 < 500\,\mu m < PS4 < 710\,\mu m.$$

The stability of the biomass was evaluated at different pHs (in the target pH range of the study; i.e., between 2 and 6.5). With some brown algae, some compounds may be dissolved during metal sorption causing potential "re-precipitation" phenomena [12]. In such a case a pre-treatment with calcium chloride is necessary. The biomass was stabilized at target pH values, the filtrate was recovered and mixed with metal solutions in order to verify the occurrence of precipitation. In the present case, the biomass was stable and could be used without any treatment.

In order to characterize the biomass, the biopolymers were extracted using the procedure described by Pereira et al. [21]. The treatment consists in rehydrating the biomass for 12 h in water before a treatment with a 1:1 acetone/methanol mixture. The biomass is digested in 150 mL of a 1 M NaOH solution at 80 °C under reflux for 3 h. Finally, the suspension is filtrated and the filtrate (containing the characteristic biopolymers) is precipitated by the addition of ethanol (96%). The precipitate was dried and analyzed by FT-IR spectrometry (FT-IR Bruker equipped with OPUS Software) after inclusion in KBr discs.

SEM-EDAX analysis was also performed on the biomass for observation and identification of binding localization. The dry sorbent was analyzed using an Environmental Scanning Electron Microscopy (ESEM) Quanta FEG 200, equipped with an OXFORD Inca 350 Energy Dispersive X-ray microanalysis (EDX) system.

2.2. Sorption experiments

The influence of pH was studied by contact for 48 h of the biosorbent (m: 20 mg of the biosorbent at the particle size PS3) with a volume V (L) of 0.15 L of the metal solution (initial concentration, C_0: 70 mg metal L^{-1}) at target pH values. For Pb(II), initial pH was set between 2.0 and 5.5 while for Cd(II) the pH was varied between 2.0 and 7.0. The pH was controlled using molar solutions of HCl and NaOH. After 2 days of agitation on a reciprocal shaker, the solution was filtrated using a 1–2 μm pore size filtration membrane and the filtrate was analyzed by ICP-AES for equilibrium metal concentration (C_{eq}: mg metal L^{-1} or mmol metal L^{-1}) using a Jobin-Yvon Activa-M (Jobin-Yvon, Longjumeau, France). The mass balance equation was used for calculating the sorption capacity q (mg metal g^{-1}, or mmol metal g^{-1}): $q = (C_0 - C_{eq})V/m$. The final pH was systematically monitored at equilibrium.

Sorption isotherms were performed at pHs 4 and 5 for Pb(II), and pH 4 for Cd(II). A given amount of sorbent (i.e., 20, 30 or 40 mg of biosorbent, PS3) was dropped into 150 mL of metal solution at the appropriate pH. The metal concentration was varied between 5 and 200 mg metal L^{-1}. The isotherms obtained with different amounts of biosorbent were merged. The suspension was maintained under agitation for 24 h using a reciprocal shaker at room temperature (i.e., 20 ± 1 °C). Finally, the suspension was filtrated and the residual concentration of metal was analyzed by ICP-AES. Similar procedure was used for the investigation of metal sorption in binary solutions.

Uptake kinetics was determined at room temperature mixing 1 L of solution with a fixed amount of sorbent. Samples were collected at different contact times, filtrated and analyzed by ICP-AES for the determination of the kinetic profile (plotting the relative concentration $C(t)/C_0$ versus time). The amount of sorbent (i.e., sorbent dosage, SD, g L^{-1}), the initial metal concentration and the particle size (PS1–PS4) were varied: relevant experimental conditions are extensively described in the caption of the figures.

The models used for the description of sorption isotherms and uptake kinetics are fully described in the Additional Material section.

3. Results and discussion

3.1. Characterization of biosorbent

The biomass of *C. chamissoi* was treated by the alkaline procedure for carrageenan extraction [21] and the FT-IR spectrum of the extract was compared to the spectra of κ- and ι-carrageenan (Table 1 and Fig. AM2 in the Additional Material section). The most interesting wavenumbers for carrageenan identification range between 1400 and 700 cm^{-1} [19]. The bands appearing on the spectrum of the alkaline extract are consistent with those identified on κ- and ι-carrageenan and reported by Pereira et al. [19]. The peak at 801 cm^{-1} is typical of ι-carrageenan (also reported for θ-carrageenan). This peak did not appear on the spectrum of the alkaline extract of *C. chamissoi*. This probably means that the alga is mainly constituted of κ-carrageenan (or its precursor μ-carrageenan). This is consistent with the levels (molar fraction of κ-carrageenan) reported for several species of *Chondracanthus* algae (50–82 mol%) [27] and more specifically for *C. chamissoi* (82 mol%)[28].

The SEM analysis of the sorbent showed different structures such as tubular forms and more massive shapes. The surface of the biosorbent is quite irregular (stripped forms). The cross-sections of the tubes show irregular or heterogeneous aspects. The SEM-EDX analysis allows identifying the presence of major elements (Fig. AM3, Additional Material section). The most representative elements are alkaline and alkaline earth metals, the sulfur element (sulfated polysaccharides) and the target sorbed metals (i.e., Pb and Cd). Actually, it was not possible detecting significant variations in the distribution of S and Pb (or Cd) for the different samples. The biosorbent can be roughly considered as a homogeneous material in terms of metal sorption.

Table 1
FT-IR analysis of alkaline extract of *C. chamissoi* biomass and identification of main characteristic peaks for κ- and ι-carrageenan.

Wavenumbers (cm^{-1})[a]	Bond[a]	Reactive group[a]	κ-car[a]	ι-car[a]	Alkaline extract of *C. chamissoi* (cm^{-1})[b]
1240–1260	S=O	Sulfate ester	+	++	1250.5
1070	C–O	3,6-Anhydrogalactose	+	+	1071.5
970–975		Galactose	+	+	Poorly resolved
930	C–O	3,6-Anhydrogalactose	+	+	929.6
845	C–O–SO_3	On C4 of galactose	+	+	833.3 [844.0 (κ-) and 838.6 (ι-)]
805	C–O–SO_3	On C2 of 3,6-anhydrogalactose	–	+	[801.2 (ι-)]

[a] From Pereira et al. [19].
[b] Into brackets the wavenumbers for κ- and ι-carrageenan on FT-IR spectra (present work).

3.2. Influence of pH

The pH of the solution may affect sorption through different effects or mechanisms: (a) influence on metal speciation, (b) biomass degradation, and (c) protonation/deprotonation of reactive groups. The optimization of the pH, taking into account the characteristics of the biosorbent and those of the effluent, is thus an important preliminary step in the study of metal biosorption. Fig. 1 shows the influence of pH on Pb(II) and Cd(II) biosorption. Below pH 2 the sorption capacity remained negligible, the sorption capacity progressively increases up to pH 5. Above pH 5, the sorption capacity tends to stabilize. Experimental conditions (i.e., pH and metal concentrations) were selected for preventing metal precipitation. At low pH, the competition of protons with metal ions for binding on reactive groups may explain the negligible sorption of both Pb(II) and Cd(II). Similar trends were observed for the binding of Cd(II) on *Mastocarpus stellatus* [16]: the titration of the biomass showed a pK_a value (i.e., 1.56) close to the values corresponding to sulfated groups from galactopyranose units (i.e., between 1 and 2.5) of carrageenans and agar. The sorption was thus attributed to the carrageenan groups present in this type of algae: Bixler [28] analyzed the carrageenans present in *M. stellatus* and evaluated the molar fraction of κ-carrageenan to 74%. The increase of metal sorption with pH above pH 2 can thus be correlated to the acid–base properties of the sulfated polysaccharides present in *C. chamissoi*. Above the pK_a of sulfated polysaccharides the competition of protons decreases and sulfated groups remain available for metal binding. Above pH 5 the sorption capacity stabilized for both Pb(II) and Cd(II) binding. The sorption efficiency approached 55% and 32% under selected experimental conditions for Pb(II) and Cd(II), respectively: the sorbent was saturated at given pH.

It is also important to evaluate the impact of sorption on pH variation. Indeed, frequently the acid–base properties of the sorbent may induce proton binding, or proton release, that causes substantial variation of the pH. This pH variation may change with metal concentration, sorbent dosage, ionic strength of the solution. A substantial and variable change in the pH of the solution during the process can strongly impact the comparison of sorption performance, the interpretation of sorption mechanisms and the modeling of experimental data. The second panel of Fig. 4 shows the equilibrium pH (pH_f) as a function of initial pH (pH_i) In the case of Pb(II) the distribution of experimental data is close to the first bisector and the pH variation did not exceed 0.2 units; in the case of Cd(II) the pH variation was more marked and reached up to 0.4–0.5 pH units, especially above pH 4.5. Based on these results, the pH value was set to pH 4 for the study of sorption isotherms and uptake kinetics.

3.3. Sorption isotherms

The sorption isotherms are reported in Fig. 2. For Pb(II) the isotherms have been established for both pH 4 and pH 5 in order to evaluate the potential impact of small pH variations on the maxi-

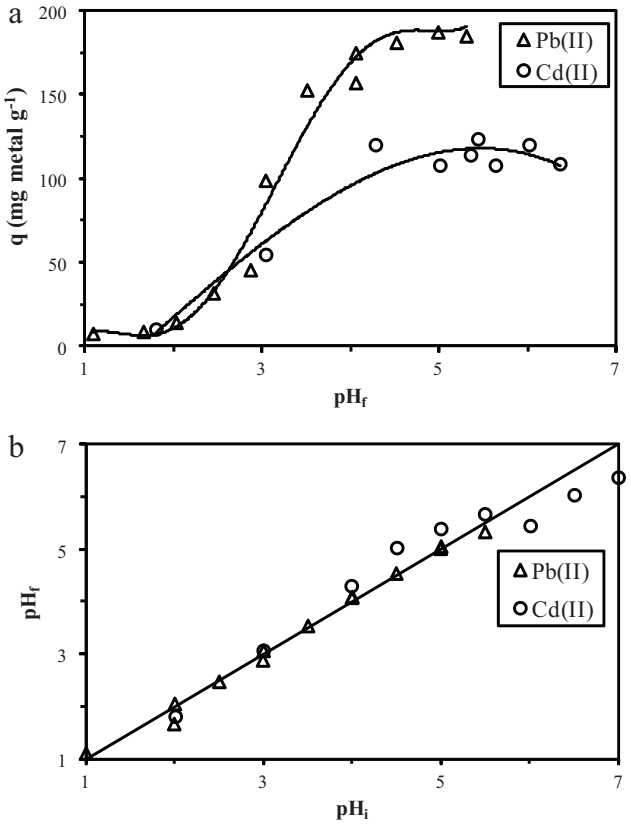

Fig. 1. Influence of pH on Pb(II) and Cd(II) sorption on *C. chamissoi* (a) and pH variation (b) during metal sorption (C_0: 70 mg metal L^{-1}; PS: 250–500 μm; SD: 0.2 g L^{-1}).

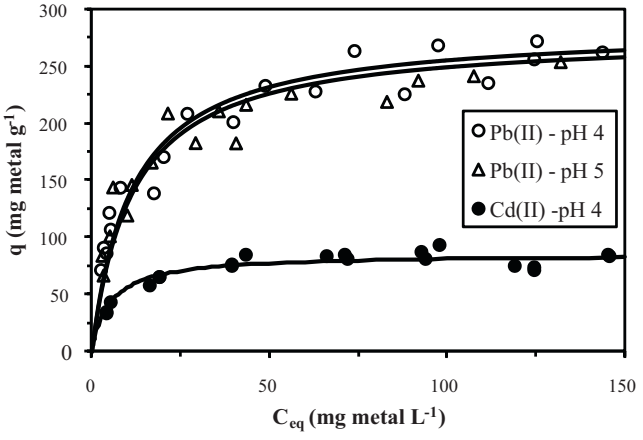

Fig. 2. Pb(II) and Cd(II) sorption isotherms on *C. chamissoi* (pH_i: 4 and 5 for Pb(II) and 4 for Cd(II)).

mum sorption capacity. The isotherms were superimposed and the pH variation did not influence sorption profile. For the isotherm at pH 5 the final pH varied between 4.9 and 5.5, while at pH 4 the final pH ranged between 3.8 and 4.3. These results confirm that for Pb(II) the final pH remained relatively stable on this pH range (pHs 4–5) and that the modeling of sorption isotherms will be meaningful. In the case of Cd(II), the isotherm was carried out at pH 4 and the final pH ranged between 4.1 and 4.3.

C. chamissoi had a preference for Pb(II) over Cd(II). The maximum sorption capacity exceeded 270 mg Pb g^{-1} (comparable for pH 4 and pH 5) against 80 mg Cd g^{-1}. The continuous lines in Fig. 2 show the modeling of the isotherms with the Langmuir equation. The parameters of the model are summarized in Table 2. The greater affinity of *C. chamissoi* for Pb(II) is confirmed by the sorption capacities at saturation of the monolayer (q_m): 277–283 mg Pb g^{-1} against 85 mg Cd g^{-1}. In molar units, the sorption capacity for Pb(II) was almost the double of the sorption capacity of Cd(II): 1.35 mmol Pb g^{-1} versus 0.76 mmol Cd g^{-1}. In terms of affinity coefficient (the *b* coefficient of the Langmuir equation), the differences are less marked. The affinity coefficient of the biosorbent was a little higher for Cd(II) than for Pb(II), but these values remain in the same order of magnitude: 21 L $mmol^{-1}$ for Cd(II) versus 18 L $mmol^{-1}$ for Pb(II). The coefficient $q_m \times b$ is representative of the initial slope of the sorption isotherm; it is slightly higher for Pb(II) (25 L g^{-1}) than for Cd(II) (16 L mg^{-1}).

It sounds interesting to correlate the higher sorption of Pb(II) (over Cd(II)) on *C. chamissoi* to their intrinsic characteristics, according to the Hard and Soft Acid and Base theory (HSAB theory) [29]. The metals can be ranked according to their electronegativity and polarizability as hard acids, borderline (such as Pb(II)) or soft acids (such as Cd(II)). Sulfate is classified as a borderline ligand (borderline base) while sulfonic groups are considered as a hard base. The softness coefficients for Cd(II), Pb(II) and sulfate groups are 0.58, 0.41 and −0.38, respectively [30]. The HSAB theory supposes that hard (Lewis) acids prefer to bind to hard (Lewis) bases (and reciprocal). Based on the hypothesis that sulfated polysaccharides are responsible for metal binding in *C. chamissoi* the preference of the biosorbent for Pb(II) can thus be explained by the greater affinity between sulfate (borderline base)/sulfonate (hard base) groups of the biosorbent for Pb(II) (borderline acid) compared to Cd(II) (soft acid).

Table 3 reports some sorption capacities of different red algae for Pb(II) and Cd(II). This table shows that *C. chamissoi* has a significantly higher sorption capacity than the red algae conventionally tested for Pb(II) and Cd(II) (with the remarkable exception of *Galaxaura marginata* when the biomass is pre-treated with HCl to remove $CaCO_3$ from this calcareous algae). The values found in the present work are quite similar to those obtained with brown algae (alginate-rich biosorbents). For Pb(II), sorption capacities ranging between 1.1 and 1.31 mmol Pb g^{-1} were obtained for *Sargassum vulgare*, *Fucus vesiculosus*, *Sargassum natans* and *Ascophyllum nodosum* at pH 3.5 [31]. For Cd(II), sorption capacities varied between 0.66 and 0.79 mmol Cd g^{-1} for several *Sargassum* species (i.e., *S. vulgare*, *S. fluitans*, *S. muticum* and *S. filipendula*) at pH 4.5 [35]. Holan et al. [36] reported higher values for Cd(II) sorption at pH 3.5 with *S. natans* and *A. nodosum* (around 1.18 mmol Cd g^{-1}), and up to 1.91 mmol Cd g^{-1} for *A. nodosum* when increasing the pH to 4.9. *C. chamissoi* is among the most efficient red algae for Pb(II) and Cd(II) biosorption but remains slightly less efficient than brown algae, especially for Cd(II) biosorption. Sulfate/sulfonic groups of carrageenans are less reactive than carboxylic groups of alginate.

In order to confirm the preference of the biosorbent for Pb(II) over Cd(II) sorption isotherms were carried out in binary solutions. The sorption of Pb(II) was tested in the presence of Cd(II) at fixed concentration (100 mg Cd L^{-1}), and reciprocally the sorption of Cd(II) was performed in the presence of Pb(II) at fixed concentration (i.e., 100 mg Pb L^{-1}) (Fig. AM4, Additional Material section). The sorption capacities for a target metal are considerably decreased in the presence of the competitor ion. Both the initial slope of the curves (correlated to the affinity of the biosorbent for the metal) and the maximum sorption capacities were decreased. The two metals compete for the same sorption sites. However, the total sorption capacity remained quite high; it varied between 0.7 and 1.12 mmol metal g^{-1} for Pb(II) in the presence of Cd(II) as the competitor metal, and between 0.76 and 0.98 mmol metal g^{-1} for Cd(II) in the presence of Pb(II). The bi-component sorption isotherms were modeled with the extended Langmuir equation (with the parameters of the isotherms in mono-component solutions, see Additional Material section, Fig. AM4). The extended Langmuir equation failed to fit experimental data in binary solutions. The two metals did not play "symmetrical" role. The relative position of the curves indicates that Pb(II) was preferentially sorbed: the Pb(II) binary isotherm curve was above the extended Langmuir simulation while the Cd(II) binary isotherm was below the simulated curve. These results confirm the preference of the biosorbent for Pb(II), although this preference is not sufficient for separating the metal ions by a single sorption step.

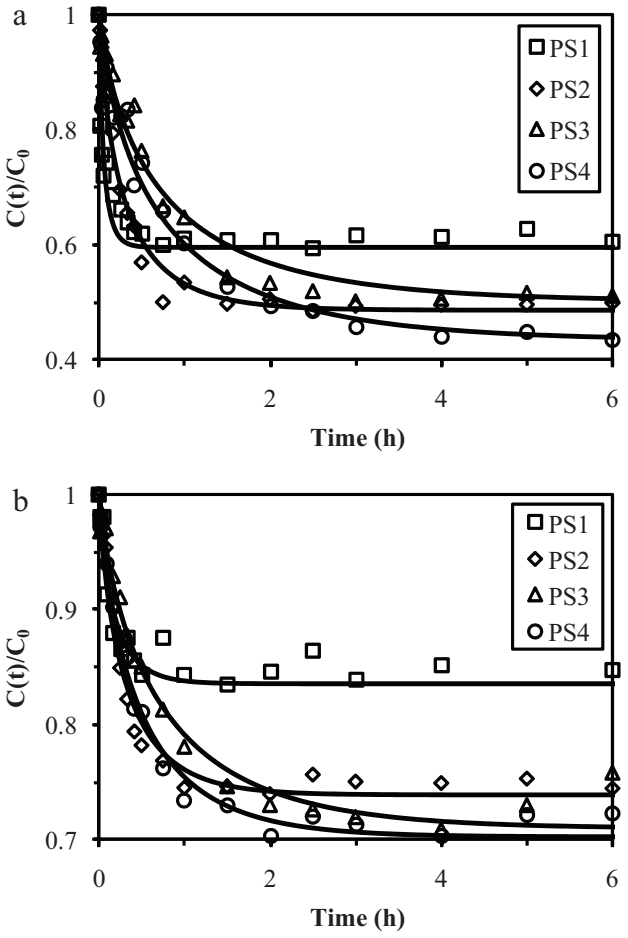

Fig. 3. Influence of particle size on Pb(II) (a) and Cd(II) (b) uptake kinetics using *C. chamissoi* (SD: 0.15 g L^{-1}; pH: 4; C_0: 50 mg metal L^{-1}; *T*: 20 °C; *v*: 250 rpm)—Modeling using the resistance to intraparticle diffusion equation.

3.4. Uptake kinetics

The uptake kinetics has been studied evaluating the influence of particle size, sorbent dosage, metal concentration and temperature (Figs. 3–5). The experimental data were modeled using the

Table 2
Sorption isotherms for *C. chamissoi*—Parameters of the Langmuir equation (particle size: PS3 250–500 μm).

Metal	pH	q_m (mg metal g^{-1})	q_m (mmol metal g^{-1})	b (L mg^{-1})	b (L $mmol^{-1}$)	R^2
Pb(II)	4	283.5	1.37	0.089	18.5	0.990
Pb(II)	5	276.7	1.34	0.088	18.2	0.974
Cd(II)	4	85.2	0.76	0.190	21.3	0.987

Table 3
Comparison of Pb(II) and Cd(II) sorption capacities for different red algae (native).

Biosorbent	Metal	pH	Sorption capacity (mmol metal g^{-1})	Reference
Chondrus crispus	Pb(II)	3.5	0.13	[31]
Galaxaura marginata	Pb(II)	3.5	0.13	[31]
Galaxaura marginata[a]	Pb(II)	3.5	1.53	[31]
Gracilaria corticata	Pb(II)	4.5	0.26	[32]
Gracilaria canaliculata	Pb(II)	4.5	0.20	[32]
Gracilaria sp.	Pb(II)	5.0	0.45	[14]
Polysiphonia violacea	Pb(II)	4.5	0.49	[32]
Chondracanthus chamissoi	Pb(II)	4–5	1.35	This study
Mastocarpus stellatus	Cd(II)	2.4	0.49	[16]
Mastocarpus stellatus	Cd(II)	4	0.56	[16]
Mastocarpus stellatus	Cd(II)	6	0.59	[16]
Hypnea valentiae	Cd(II)	6.0	0.14–0.25	[33]
Gracilaria sp.	Cd(II)	5.0	0.30	[14]
Gracilaria fisheri	Cd(II)	4.0	0.63	[34]
Chondracanthus chamissoi	Cd(II)	4	0.76	This study

[a] Calcareous algae, *Galaxaura marginata*, treated with HCl for $CaCO_3$ removal.

Table 4
Influence of particle size (PS) on uptake kinetics—Modeling of experimental data with the simplified model of resistance to intraparticle diffusion (Crank's equation) and PSORE model (SD: 0.15 g L^{-1}; C_0: 50 mg metal L^{-1}).

Metal	PS (μm)	Crank's equation		PSORE equation			
		$D_{eff} \times 10^{11}$ (m^2 min^{-1})	EV	$q_{m,exp}$ (mg metal g^{-1})	$q_{m,calc.}$ (mg metal g^{-1})	$k_2 \times 10^3$ (g mg^{-1} min^{-1})	R^2
Pb(II)	80–125	12.2	0.11	128	127	10.1	0.999
Pb(II)	125–250	6.2	0.04	167	172	0.63	0.998
Pb(II)	250–500	9.9	0.05	166	182	0.20	0.985
Pb(II)	500–710	23.5	0.10	206	222	0.19	0.989
Cd(II)	80–125	4.8	0.17	55	53	4.2	0.994
Cd(II)	125–250	8.1	0.06	87	90	1.1	0.996
Cd(II)	250–500	13.4	0.05	98	99	0.51	0.977
Cd(II)	500–710	52.5	0.03	104	105	0.72	0.994

D_{eff} (m^2 min^{-1}); $q_{m,exp}$ (mg metal g^{-1}); $q_{m,calc.}$ (mg metal g^{-1}); k_2 (g mg^{-1} min^{-1}).

pseudo-second order rate equation (PSORE, represented in the Additional Material section, Figs. AM5–AM7) and the model of resistance to intraparticle diffusion (RID, Crank equation, represented in Figs. 3–5). Tables 4–6 summarize the parameters of the two models.

Note: Some discrepancies can be observed between the equilibrium sorption capacities reported in Table 2 compared to Tables 4–6, in the case of Cd(II) biosorption. The values obtained in uptake kinetics were generally higher than the values of the parameters of the Langmuir equation. It is noteworthy that the maximum sorption capacity obtained from the Langmuir equation is a mathematical value approximated by the linearization of the equation and this may slightly vary compared to experimental values. Additionally, depending on experimental conditions

Table 5
Influence of sorbent dosage (SD, g L^{-1}) on uptake kinetics—Modeling of experimental data with the simplified models of resistance to film diffusion, intraparticle diffusion (Crank's equation) and PSORE model (PS: 250–500 μm; C_0: 50 mg metal L^{-1}).

		Film diffusion	Crank's equation		PSORE equation				
Metal	SD	k_sS	R^2	$D_{eff} \times 10^{11}$	EV	$q_{m,exp}$	$q_{m,calc.}$	$k_2 \times 10^3$	R^2
Pb(II)	0.06	0.317	0.948	16.3	0.18	230	256	0.14	0.979
Pb(II)	0.12	0.222	0.945	11.9	0.17	190	220	0.12	0.898
Pb(II)	0.15	0.227	0.975	9.9	0.05	166	182	0.20	0.985
Pb(II)	0.18	0.216	0.979	12.7	0.15	160	169	0.34	0.994
Pb(II)	0.24	0.184	0.972	11.0	0.03	137	145	0.37	0.995
Cd(II)	0.06	0.316	0.940	14.0	0.18	107	109	0.71	0.989
Cd(II)	0.12	0.219	0.949	11.6	0.17	102	106	0.70	0.993
Cd(II)	0.15	0.193	0.976	13.4	0.05	98	99	0.51	0.977
Cd(II)	0.18	0.174	0.990	9.0	0.15	93	98	0.60	0.995
Cd(II)	0.24	0.132	0.983	14.8	0.07	85	89	0.74	0.994

k_sS: min^{-1}; D_{eff} (m^2 min^{-1}); $q_{m,exp}$ (mg metal g^{-1}); $q_{m,calc.}$ (mg metal g^{-1}); k_2 (g mg^{-1} min^{-1}).

Table 6
Influence of metal concentration (C_0, mg metal L^{-1}) on uptake kinetics—Modeling of experimental data with the simplified model of resistance to intraparticle diffusion (Crank's equation) and PSORE model (SD: 0.15 g L^{-1}; particle size: 250–500 μm).

Metal	C_0	Film diffusion		Crank's equation		PSORE equation			
		k_sS	R^2	$D_{eff} \times 10^{11}$	EV	$q_{m,exp}$	$q_{m,calc.}$	$k_2 \times 10^3$	R^2
Pb(II)	15	0.184	0.999	4.5	0.07	82	97	0.20	0.974
Pb(II)	30	0.190	0.994	6.4	0.17	129	154	0.14	0.974
Pb(II)	50	0.227	0.976	9.9	0.05	166	182	0.20	0.985
Pb(II)	70	0.230	0.966	13.5	0.03	197	213	0.23	0.994
Pb(II)	100	0.234	0.952	23.1	0.02	223	233	0.38	0.998
Cd(II)	15	0.205	0.996	9.2	0.04	57	63	0.55	0.991
Cd(II)	30	0.242	0.919	15.6	0.02	81	87	0.55	0.994
Cd(II)	50	0.194	0.976	13.4	0.05	98	99	0.51	0.977
Cd(II)	70	0.213	0.944	39.3	0.02	114	115	1.45	0.998
Cd(II)	100	0.191	0.953	33.5	0.08	114	112	0.74	0.991

k_sS: min^{-1}; D_{eff} (m^2 min^{-1}); $q_{m,exp}$ (mg metal g^{-1}); $q_{m,calc.}$ (mg metal g^{-1}); k_2 (g mg^{-1} min^{-1}).

(varying metal concentration, changing sorbent dosage) may affect pH variation, which in turn can impact sorption capacity at equilibrium. In some cases (depending on experimental conditions) the residual metal concentration tended to increase at long contact time, this may contribute to a slight decrease of sorption capacity. The sorption isotherms were collected after 24 h of contact, contrary to uptake kinetics that were limited to the first 6 h of agitation. The combination of these different reasons may explain the little discrepancies observed in the tables.

3.4.1. Effect of particle size

The particle size is a critical parameter for the kinetics of sorption processes. Indeed, the size of sorbent influences the external surface area available for interacting with the solution through the effect on the resistance to film diffusion. Additionally, the particle radius may influence the time required for solute to diffuse to the center of the sorbent particle (resistance to intraparticle diffusion). When the porosity of the material is very small the diffusion of large solute molecule may be strictly hindered and the sorption can be limited to external sorbent layers. In this case the sorption capacity can decrease when increasing the size of sorbent parti-

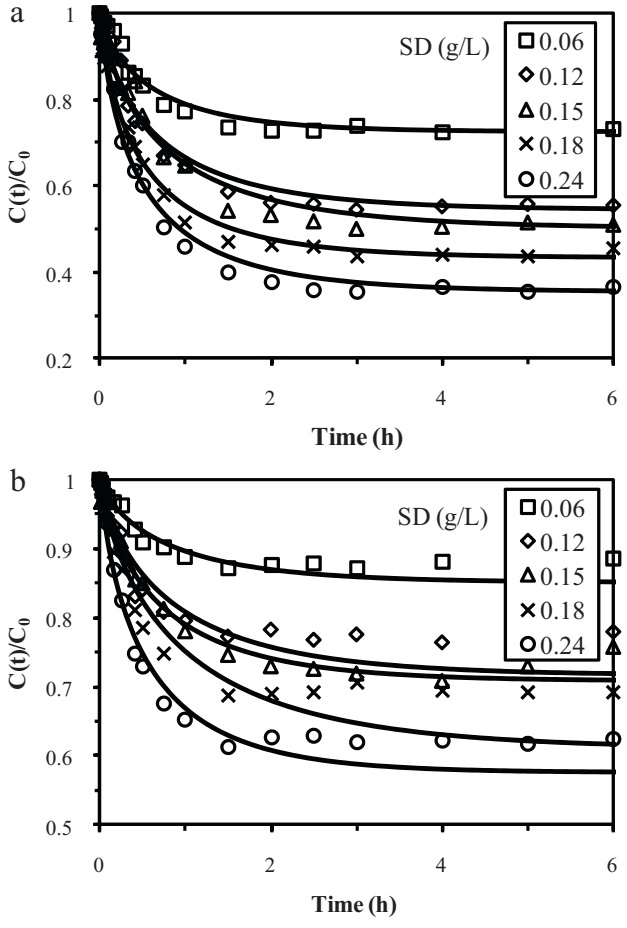

Fig. 4. Influence of sorbent dosage (g L^{-1}) on Pb(II) (a) and Cd(II) (b) uptake kinetics using *C. chamissoi* (SD: Influence of sorbent dosage (SD g L^{-1}); PS: 250–500 μm; pH: 4; C_0: 50 mg metal L^{-1}; *T*: 20 °C; *v*: 250 rpm)—Modeling using the resistance to intraparticle diffusion equation.

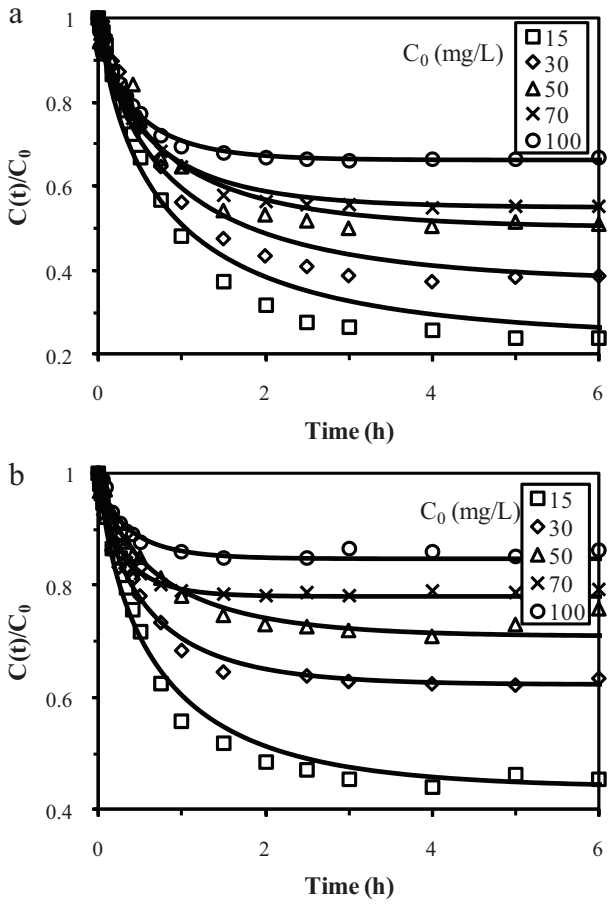

Fig. 5. Influence of metal concentration (C_0: mg L^{-1}) on Pb(II) (a) and Cd(II) (b) uptake kinetics using *C. chamissoi* (PS: 250–500 μm; pH: 4; SD: 0.15 g L^{-1}; *T*: 20 °C; *v*: 250 rpm)—Modeling using the resistance to intraparticle diffusion equation.

cles. In the case of *C. chamissoi* the residual concentration tended to increase with decreasing particle size (Fig. 3). This is contrary to the expected trend. A similar decrease of sorption capacity with decreasing particle size was also cited in the case of uranyl sorption using *Catenella repens* (a red alga) [15]. Bhat et al. [15] suggested that the grinding of the biosorbent to reach small-size particles can induce damages to reactive groups that decrease their availability and activity. In the case of Pb(II), the decrease in sorption efficiency seems to be more proportional than in the case of Cd(II), for which a large difference was only observed between PS1 and other samples. The particle size PS3 was used for the investigation of other parameters.

The intraparticle diffusivity significantly increased with increasing particle size by a factor 4–11 (Table 4). For a homogeneous porous material the variation would be much lower; in the present case this large variation is probably related to the effect of biosorbent modification (due to grinding operation as suggested above). The intraparticle diffusivity for Pb(II) was slightly higher than the values obtained for Cd(II). This can be probably explained by the fact that the ionic radius of Pb(II) (i.e., 118 pm) is slightly greater than the ionic radius of Cd(II) (i.e., 95 pm). The molecular diffusivities (D_0) for Pb(II) and Cd(II) are $5.67 \times 10^{-8}\,m^2\,min^{-1}$ and $4.31 \times 10^{-8}\,m^2\,min^{-1}$, respectively [30]. This is about 3 orders of magnitude higher than the values reached for intraparticle diffusivities. The PSORE model slightly overestimated the equilibrium sorption capacity, especially for Pb(II). The kinetic rate constant (k_2) decreased with increasing the size of sorbent particles, especially for PS1 and PS2 particles, for largest particles the impact of the size of the sorbent on the kinetic parameter was less marked. A similar trend was observed for the sorption of Hg(II) using two kelps (*Lessonia nigrescens* and *Lessonia trabeculata*) [12].

3.4.2. Effect of sorbent dosage

Fig. 4 shows the effect of sorbent dosage on the kinetic profiles (see also Fig. AM6, in Additional Material section). Obviously, the variation of sorbent dosage affects the equilibrium concentration. Table 5 reports the coefficients of the kinetic models. The values of the intraparticle diffusion coefficient varied around $1.2 \times 10^{-10}\,m^2\,min^{-1}$ for Pb(II) and around $1.3 \times 10^{-10}\,m^2\,min^{-1}$ for Cd(II). It was not possible detecting a clear trend for the evolution of the intraparticle diffusivity when varying the sorbent dosage. The resistance to intraparticle diffusion is controlled by the porosity characteristics of the sorbent, which are not expected to vary with sorbent dosage. In some cases, the variation of the sorbent dosage influences the concentration gradient between the solution and the internal reactive groups. This could be due to a strong sorption of the solute at the external sorbent surface; the decrease of the concentration gradient and of the driving force influence the intraparticle diffusion. This is not the case in the present system. These experiments were carried out using the PS3 size for which the sorption isotherm was investigated. It is thus possible evaluating the film diffusion rate (k_fS) (see Additional Material section). The film diffusion rate decreased with increasing the sorbent dosage (Table 5).

The characteristics of biosorbent particles (apparent density and particle porosity, ρ_p and ε_p) were not determined; it is thus impossible calculating the specific outside surface (S) and then the film diffusion coefficient (k_f). In the case of *S. fluitans*, Leusch and Volesky determined the specific characteristics of the biomass (apparent density: $0.53\,g\,mL^{-1}$; porosity: 0.43) [37]. These parameters were used for approaching the value of the coefficient S for the different SD values: 3.2, 6.4, 8.0, 9.5 and $12.7\,m^{-1}$ (for SD: 0.06, 0.12, 0.156, 0.18 and 0.24, respectively) and to deduce an approximate value of the film diffusion coefficient for both Pb(II) and Cd(II). For SD varying between 0.12 and $0.24\,g\,L^{-1}$, the k_f coefficient linearly decreased with increasing SD in the range $1.4 \times 10^{-5}\,m\,min^{-1}$ and $3.5 \times 10^{-5}\,m\,min^{-1}$ for Pb(II) and between $1.0 \times 10^{-5}\,m\,min^{-1}$ and $3.4 \times 10^{-5}\,m\,min^{-1}$ for Cd(II). For the smallest SD ($0.06\,g\,L^{-1}$), the value of the coefficient was much higher (around $9.9 \times 10^{-5}\,m\,min^{-1}$ for both Pb(II) and Cd(II)). Though these values must be considered as approximations of k_f, they can be used to compare the respective contributions of the resistance to film diffusion and to intraparticle diffusion through the calculation of the Biot number:

$$\text{Biot number}: N_{Biot} = \frac{k_f r}{D_{eff}} \quad (1)$$

When $N_{Biot} \gg 1$ the resistance to film diffusion can be considered negligible compared to the resistance to intraparticle diffusion [38]. In the present case, even under the less "favorable" conclusion (highest D_{eff} and lowest k_f), the Biot number exceeded 10. This is an indication that the intraparticle diffusion resistance will be the predominant limiting mechanism for both Pb(II) and Cd(II) uptake.

The PSORE model was also applied (Table 5): the sorbent dosage hardly influenced the k_2 coefficient for Pb(II) (varying between 0.12×10^{-3} and $0.34 \times 10^{-3}\,g\,mg^{-1}\,min^{-1}$) and Cd(II) (varying between 0.51×10^{-3} and $0.74 \times 10^{-3}\,g\,mg^{-1}\,min^{-1}$).

3.4.3. Effect of metal concentration

The uptake kinetics was compared for different initial metal concentrations (Fig. 5 and Fig. AM7, in the Additional Material section). The values of the parameters for the different models are summarized in Table 6. The film diffusion rate coefficient varied between 0.184 and $0.234\,min^{-1}$ for Pb(II) and between 0.191 and $0.242\,min^{-1}$ for Cd(II). The intraparticle diffusion coefficient increased with metal concentration by a factor 4–5 for Pb(II) and Cd(II). This effect on the resistance to intraparticle diffusion is probably due to the positive effect of increasing metal concentration on the concentration gradient between the solution and the internal reactive groups. Increasing metal concentration enhanced the driving force and improved mass transfer. However, the differences are not very marked. The dependence of the intraparticle diffusion coefficient on solute concentration has been discussed. Hence, Nestle and Kimmich [39], in the case of metal binding on alginate gels, correlated the evolution of the intraparticle diffusion coefficient with metal concentration according to the sorption isotherm. This dependence of the intraparticle diffusion coefficient with solute concentration, in the case of a Langmuir-type isotherm, follows the equation:

$$D_{eff}(C) = \frac{(1+bC)^2}{(1+bC)^2 + bq_m} D_0 \quad (2)$$

This relationship was verified in the case of Pb(II) using the equilibrium concentrations for the calculation of the effective diffusivity. The comparison of calculated and experimental intraparticle diffusivities shows a linear trend:

$$D_{exp.} = 0.53 \times D_{calc.} + 2 \times 10^{-11} \quad (R^2 = 0.966) \quad (3)$$

In the case of Cd(II) it was not possible correlating the intraparticle diffusion coefficient with residual equilibrium concentrations.

4. Conclusion

The biomass of *C. chamissoi*, a κ-carrageenan-rich alga, can be successfully used for the biosorption of Pb(II) and Cd(II). Maximum sorption capacities ($1.37\,mmol\,Pb\,g^{-1}$ and $0.76\,mmol\,Cd\,g^{-1}$ at pH 4) are comparable to those of brown algae and higher than the levels reached with the red algae that were previously tested for the sorption of these metal ions. The preference for Pb(II) over Cd(II) can be explained by the difference in the higher affinity of sulfated polysaccharides for Pb(II) (HSAB rules).

Uptake kinetics is controlled by the resistance to intraparticle diffusion. The uptake profiles were also successfully modeled by the pseudo-second order rate equation. The intraparticle diffusivity coefficient was about 3 orders of magnitude lower than the molecular diffusivity of Pb(II) and Cd(II) in water. The sorbent dosage hardly influenced the intraparticle diffusivity and the pseudo-second order rate coefficients. The impact of metal concentration and particle size was a little more marked.

This strong affinity of *C. chamissoi*, can be used for metal recovery from waste streams, but it should be also taken into account for the production of carrageenan. Indeed, *C. chamissoi* is part of the algae that are commercially exploited for the industrial production of this important polysaccharide used in food industry. The growth/collect of algae in areas submitted to heavy metal discharge may induce the production of contaminated biopolymers. It is thus important to analyze the biomass before the extraction of polysaccharides. A pre-treatment (metal desorption) can be necessary using an acidic treatment [16], or an alkaline treatment depending on the chemistry of metals ions and their interaction mode with the biomass.

Acknowledgements

Authors thanks European Union for financial support under the ALFA program (Contract AML/190901/06/18414/II-0548-FC-FA), and the Program PREPA-PREFALC (for supporting the collaboration between Ecole des Mines d'Alès and the Universidad Peruana Cayetano Heredia).

Appendix A. Supplementary data

Supplementary data associated with this article can be found, in the online version, at doi:10.1016/j.jhazmat.2010.09.108.

References

[1] M.M. Matlock, B.S. Howerton, D.A. Atwood, Irreversible precipitation of mercury and lead, J. Hazard. Mater. B 84 (2001) 73–82.
[2] B.R. Reddy, D.N. Priya, Chloride leaching and solvent extraction of cadmium, cobalt and nickel from spent nickel–cadmium, batteries using Cyanex 923 and 272, J. Power Sources 161 (2006) 1428–1434.
[3] M.E. Malla, M.B. Alvarez, D.A. Batistoni, Evaluation of sorption and desorption characteristics of cadmium, lead and zinc on Amberlite IRC-718 iminodiacetate chelating ion exchanger, Talanta 57 (2002) 277–287.
[4] R. Navarro, I. Saucedo, A. Nunez, M. Avila, E. Guibal, Cadmium extraction from hydrochloric acid solutions using Amberlite XAD-7 impregnated with Cyanex 921 (tri-octyl phosphine oxide), React. Funct. Polym. 68 (2008) 557–571.
[5] M.A. Dubois, J.F. Dozol, C. Nicotra, J. Serose, C. Massiani, Pyrolysis and incineration of cationic and anionic ion-exchange resins—Identification of volatile degradation compounds, J. Anal. Appl. Pyrol. 31 (1995) 129–140.
[6] B. Volesky, Z.R. Holan, Biosorption of heavy metals, Biotechnol. Prog. 11 (1995) 235–250.
[7] L. Svecova, M. Spanelova, M. Kubal, E. Guibal, Cadmium, lead and mercury biosorption on waste fungal biomass issued from fermentation industry. 1. Equilibrium studies, Sep. Purif. Technol. 52 (2006) 142–153.
[8] G. Bayramoglu, I. Tuzun, G. Celik, M. Yilmaz, M.Y. Arica, Biosorption of mercury(II), cadmium(II) and lead(II) ions from aqueous system by microalgae *Chlamydomonas reinhardtii* immobilized in alginate beads, Int. J. Miner. Process. 81 (2006) 35–43.
[9] B. Cordero, P. Lodeiro, R. Herrero, M.E.S. de Vicente, Biosorption of cadmium by *Fucus spiralis*, Environ. Chem. 1 (2004) 180–187.
[10] A. Fraile, S. Penche, F. Gonzalez, M.L. Blazquez, J.A. Munoz, A. Ballester, Biosorption of copper, zinc, cadmium and nickel by *Chlorella vulgaris*, Chem. Ecol. 21 (2005) 61–75.
[11] P. Lodeiro, B. Cordero, J.L. Barriada, R. Herrero, M.E.S. de Vicente, Biosorption of cadmium by biomass of brown marine macroalgae, Bioresour. Technol. 96 (2005) 1796–1803.
[12] M. Reategui, H. Maldonado, M. Ly, E. Guibal, Mercury(II) biosorption using *Lessonia sp*. kelp, Appl. Biochem. Biotechnol. 162 (2010) 805–822.
[13] A. Seker, T. Shahwan, A.E. Eroglu, S. Yilmaz, Z. Demirel, M.C. Dalay, Equilibrium, thermodynamic and kinetic studies for the biosorption of aqueous lead(II), cadmium(II) and nickel(II) ions on *Spirulina platensis*, J. Hazard. Mater. 154 (2008) 973–980.
[14] P.X. Sheng, Y.P. Ting, J.P. Chen, L. Hong, Sorption of lead, copper, cadmium, zinc, and nickel by marine algal biomass: characterization of biosorptive capacity and investigation of mechanisms, J. Colloid Interface Sci. 275 (2004) 131–141.
[15] S.V. Bhat, J.S. Melo, B.B. Chaugule, S.F. D'Souza, Biosorption characteristics of uranium(VI) from aqueous medium onto *Catenella repens*, a red alga, J. Hazard. Mater. 158 (2008) 628–635.
[16] R. Herrero, P. Lodeiro, R. Rojo, A. Ciorba, P. Rodriguez, M.E.S. de Vicente, The efficiency of the red alga *Mastocarpus stellatus* for remediation of cadmium pollution, Bioresour. Technol. 99 (2008) 4138–4146.
[17] E. Romera, F. Gonzalez, A. Ballester, M.L. Blazquez, J.A. Munoz, Biosorption of Cd, Ni, and Zn with mixtures of different types of algae, Environ. Eng. Sci. 25 (2008) 999–1008.
[18] A. Sari, M. Tuzen, Biosorption of cadmium(II) from aqueous solution by red algae (*Ceramium virgatum*): equilibrium, kinetic and thermodynamic studies, J. Hazard. Mater. 157 (2008) 448–454.
[19] L. Pereira, A.M. Amado, A.T. Critchley, F. van de Velde, P.J.A. Ribeiro-Claro, Identification of selected seaweed polysaccharides (phycocolloids) by vibrational spectroscopy (FTIR-ATR and FT-Raman), Food Hydrocolloids 23 (2009) 1903–1909.
[20] L. Pereira, J.F. Mesquita, Carrageenophytes of occidental Portuguese coast: 1. Spectroscopic analysis in eight carrageenophytes from Buarcos bay, Biomol. Eng. 20 (2003) 217–222.
[21] L. Pereira, A. Sousa, H. Coelho, A.M. Amado, P.J.A. Ribeiro-Claro, Use of FTIR, FT-Raman and (13)C NMR spectroscopy for identification of some seaweed phycocolloids, Biomol. Eng. 20 (2003) 223–228.
[22] R.L. Veroy, N. Montano, M.L.B. Deguzman, E.C. Laserna, G.J.B. Cajipe, Studies on the binding of heavy-metals to algal polysaccharides from Philippine seaweeds. 1. Carrageenan and the binding of lead and cadmium, Bot. Mar. 23 (1980) 59–62.
[23] C.R. Bulboa, J.E. Macchiavello, E.C. Oliveira, E. Fonck, First attempt to cultivate the carrageenan-producing seaweed *Chondracanthus chamissoi* (C. Agardh) Kutzing (Rhodophyta; Gigartinales) in Northern Chile, Aquacult. Res. 36 (2005) 1069–1074.
[24] A.H. Buschmann, J.A. Correa, R. Westermeier, M.D. Hernandez-Gonzalez, R. Norambuena, Red algal farming in Chile: a review, Aquaculture 194 (2001) 203–220.
[25] J.A. Vasquez, J.M.A. Vega, *Chondracanthus chamissoi* (Rhodophyta, Gigartinales) in northern Chile: ecological aspects for management of wild populations, J. Appl. Phycol. 13 (2001) 267–277.
[26] S. Andrade, M.H. Medina, J.W. Moffett, J.A. Correa, Cadmium–copper antagonism in seaweeds inhabiting coastal areas affected by copper mine waste disposals, Environ. Sci. Technol. 40 (2006) 4382–4387.
[27] F. van de Velde, Structure and function of hybrid carrageenans, Food Hydrocolloids 22 (2008) 727–734.
[28] H.J. Bixler, Recent developments in manufacturing and marketing carrageenan, Hydrobiologia 327 (1996) 35–57.
[29] R.G. Pearson, Hard and soft acids and bases, J. Am. Chem. Soc. 85 (1963) 3533–3539.
[30] Y. Marcus, Ion Properties, Marcel Dekker, Inc., New York, NY, 1997.
[31] Z.R. Holan, B. Volesky, Biosorption of lead and nickel by biomass of marine algae, Biotechnol. Bioeng. 43 (1994) 1001–1009.
[32] R. Jalali, H. Ghafourian, Y. Asef, S.J. Davarpanah, S. Sepehr, Removal and recovery of lead using nonliving biomass of marine algae, J. Hazard. Mater. 92 (2002) 253–262.
[33] A. Rathinam, B. Maharshi, S.K. Janardhanan, R.R. Jonnalagadda, B.U. Nair, Biosorption of cadmium metal ion from simulated wastewaters using *Hypnea valentiae* biomass: a kinetic and thermodynamic study, Bioresour. Technol. 101 (2010) 1466–1470.
[34] Y. Chaisuksant, Biosorption of cadmium(II) and copper(II) by pretreated biomass of marine alga *Gracilaria fisheri*, Environ. Technol. 24 (2003) 1501–1508.
[35] T.A. Davis, B. Volesky, R.H.S.F. Vieira, *Sargassum* seaweed as biosorbent for heavy metals, Water Res. 34 (2000) 4270–4278.
[36] Z.R. Holan, B. Volesky, L. Prasetyo, Biosorption of Cd by biomass of marine algae, Biotechnol. Bioeng. 41 (1993) 819–825.
[37] A. Leusch, B. Volesky, The influence of film diffusion on cadmium biosorption by marine biomass, J. Biotechnol. 43 (1995) 1–10.
[38] C. Tien, Adsorption Calculations and Modeling, Butterworth-Heinemann, Newton, MA, 1994.
[39] N. Nestle, R. Kimmich, Concentration-dependent diffusion coefficients and sorption isotherms. Application to ion exchange processes as an example, J. Phys. Chem. 100 (1996) 12569–12573.